IEIE Transactions on Smart Processing and Computing, vol. 4, no. 5, October 2015
http://dx.doi.org/10.5573/IEIESPC.2015.4.5.311

3D Non-Rigid Registration for Abdominal PET-CT and MR Images Using Mutual Information and Independent Component Analysis

Hakjae Lee[1,2], Jaehee Chun[1], Kisung Lee[1,3]*, and Kyeong Min Kim[4]

[1] Department of Bio-convergence Engineering, Korea University / Seoul, South Korea
[2] Research Institute of Global Health Tech., Korea University / Seoul, South Korea
[3] School of Biomedical Engineering, Korea University / Seoul, South Korea
[4] Molecular Imaging Research Center Korea Institute of Radiological & Medical Sciences / Seoul, South Korea

***** Corresponding Author: Kisung Lee

Received October 14, 2015; Revised October 21, 2015; Accepted October 25, 2015; Published October 31, 2015

** Regular Paper*

***Abstract*:** The aim of this study is to develop a 3D registration algorithm for positron emission tomography/computed tomography (PET/CT) and magnetic resonance (MR) images acquired from independent PET/CT and MR imaging systems. Combined PET/CT images provide anatomic and functional information, and MR images have high resolution for soft tissue. With the registration technique, the strengths of each modality image can be combined to achieve higher performance in diagnosis and radiotherapy planning. The proposed method consists of two stages: normalized mutual information (NMI)-based global matching and independent component analysis (ICA)-based refinement. In global matching, the field of view of the CT and MR images are adjusted to the same size in the preprocessing step. Then, the target image is geometrically transformed, and the similarities between the two images are measured with NMI. The optimization step updates the transformation parameters to efficiently find the best matched parameter set. In the refinement stage, ICA planes from the windowed image slices are extracted and the similarity between the images is measured to determine the transformation parameters of the control points. B-spline–based freeform deformation is performed for the geometric transformation. The results show good agreement between PET/CT and MR images.

***Keywords*:** Image registration, Particle swarm optimization, PET/CT, MR, Independent component analysis

1. Introduction

Image registration has been widely used for various clinical applications. In particular, registration between different imaging modalities, e.g., computed tomography (CT), positron emission tomography (PET), magnetic resonance (MR), ultrasound, etc., is useful for more precisely diagnosing disease [1].

Recently, based on increases in cancer patients and advancements in imaging technologies, the demand for multimodality imaging systems has grown rapidly. The combined PET/CT system is the first multimodality imaging system that improves early detection of tumor volumes. With an anatomic image from CT and a functional image from a PET scan, oncologists can deduce the precise location of the tumor [2].

The combined PET/CT system, which can obtain both PET and CT images sequentially, shares the patient bed so the movement of the patient is minimized (this is a problematic parameter for registration). However, many studies report that registration of PET and CT images from the combined scanner is still required to some extent [3].

MR images produce better quality soft tissue images and fewer artifacts caused by metallic implants than CT images [4]. These advantages encouraged many researchers to develop PET/MR systems [5]. However, the conventional PET system has used a photo multiplier tube (PMT) as its detector, which is not compatible with the strong magnets in MR. This incompatibility requires an alternative method, and stand-alone PET and MR systems

may eliminate these physical problems.

In the Korea Institute of Radiological & Medical Sciences (KIRAMS), each of the combined PET/CT and stand-alone MR systems were set up independently in adjacent rooms. PET/CT and MR images of a patient were obtained sequentially so the time difference between each image could be minimized. The difference between the patient beds for each system creates a difference in the patient position, so software-based image registration is important in order to match the information.

There are many methods for image registration. Manual registration is achieved by finding the same anatomic structures in both images. This is performed by clinical experts, so it is slow and tedious and generally corrects only for rigid misalignments. A software-based automatic approach helps to get more accurate results by implementing elastic image registration [3, 22, 23]. This approach is being studied by various research groups, and the effectiveness of the mutual information (MI)-based voxel method has been reported in many journals [1, 9, 11]. In these papers, most of the applications were brain images where the relatively simple rigid body model can be applied. Moreover, for the hierarchical (pyramid) registration method, which is generally used for block-wise 3D registration, MI had some limitations when the size of the image block became small. In addition, the discon-tinuity between the adjacent sub-blocks due to the different transformation parameters is also problematic. So we need to develop an additional registration algorithm that can make up for the weak points of the conventional method.

Registration for brain images is usually solved by rigid body transformation because the brain is located inside the skull [15]. For abdomen registration, the organs are too flexible to be addressed with the same method, because they are non-rigidly transformed by the breath and position of the patient [6, 7]. Abdomen registration needs a more complex approach than brain registration, which requires only a simple transformation. For these reasons, and to get more precise abdominal registration results, we studied a salient feature-based registration method to overcome the drawbacks of the conventional method described above. As a method to extract features, independent component analysis (ICA) was explored. To improve the performance of the voxel method, particle swarm optimization (PSO) and GPU-based parallel processing was employed.

The objective of this study is to develop an image registration algorithm for abdominal PET/CT and MR images that are acquired separately but sequentially. We report here the proposed 3D image registration algorithm and its experimental results.

2. MATERIALS AND METHODS

The proposed algorithm consists of two stages: normalized mutual information (NMI)-based global matching and ICA-based refinement. A CT image acquired by PET/CT was used as a reference image. An MR image was used as a target image that was geometrically transformed to be compared with the reference image. After registration between CT and MR, the PET image was laid on the transformed MR image so that we achieved an aligned PET/MR image. In this method, we neglect the difference between the PET and CT images, which were taken with the patient using the same patient couch.

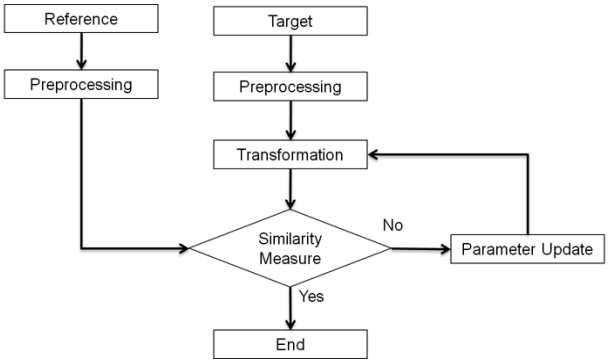

Fig. 1. Block diagram of NMI-based global matching.

2.1 NMI-based Global Matching

The goal of this stage is to roughly match the images with the global information of the CT and MR images. The global registration stage consists of four steps (preprocessing, geometric transformation, similarity measure, and optimization).

First, in the preprocessing step, the data type and size of images from different systems are adjusted to a predetermined dimension. To extract the abdominal field of view (FOV) from the whole-body images, we clipped each image from the upper side of the lungs to the femoral heads manually. The clipped CT, PET, and MR images were transformed to fit into the predetermined system volume (128 × 128 × 128 voxels). In addition, a histogram equalization method was used to make two image sets have equivalent contrast [8].

In the transformation step, the target image was transformed by a 3D affine model. Translation, rotation, and scaling were performed with nine transformation parameters. While transforming the 3D target image, we used cubic linear interpolation, which is faster than spline-based interpolation and generates smoother images than nearest neighbor interpolation.

The transformed target image (CT) was compared with the reference image (MR) by quantifying the difference between the two images in the similarity measurement step. For the similarity figures, we investigated normalized mutual information (NMI) [10, 11], the mean absolute difference (MAD), and the correlation coefficient [12, 23]. We found that NMI performed better than the other methods for multimodality images [24].

Finally, the optimization step updates the transformation parameters so that the next iteration can produce better similarity. These steps are repeated until the metric converges within the predetermined range of difference from the previous iteration. In practice, the optimization step accelerates the algorithm significantly, compared to the greedy search approach. By updating the transformation parameters effectively, it helps us to find the optimal transformation parameter set without investigating all com-

binations of the parameters. We employed a particle swarm optimization (PSO) algorithm that was inspired by social behavior of birds flocking and fish schooling [13, 14].

PSO is based on an algorithm that assumes intelligent particles share their own results, and by updating the next movements of particles with the following equation:

$$V = W \times V + C_1 \times rand() \times PBest + C_2 \times rand() \times GBest \quad (1)$$

where V is the velocity of a particle, *rand*() is a random function, *PBest* is the best value of the present step, *GBest* is the global best value of the swarm, and W, C_1, and C_2 are weight factors.

We adopted this optimization to find the parameter set of the transformation, which maximizes the similarity function. By doing these steps recursively, the best set of the transformation parameters that produces maximum NMI values is determined. Weight factors can affect the convergence time of the algorithm and the possibility of local minimum problems. In this study, the weights were empirically chosen via experimentation with a variety of data sets (W = 1.0, C_1 = 0.7, and C_2 = 1.0).

2.2 ICA-based Refinement

In this stage, we developed a feature-based registration model to improve the results of NMI-based global matching. In the global matching step, we transformed the target image via the affine transformation model so that we get generally matched abdominal CT and MR images. As we mentioned above, this conventional method, needs improvement. To supplement the limitations of the conventional intensity-based methods, we explored an additional step, which extracts features based on indepen-dent component analysis followed by elastic trans-formation [15-18].

To extract the feature information, we employed ICA, which is commonly used for blind source separation in signal processing and face detection in computer vision. ICA is a statistical method to extract components from the multidimensional random vector by maximizing the independence of each component [19, 20].

ICA is given by

$$y = Mx + l \quad (2)$$

where y is the mixed signal vector, x is the independent components of y, l is noise, and M is the estimating matrix. Even though noise l is discarded, the estimation of M and x is difficult, because we only know the y vector. However, using a condition where the x vector consists of independent elements, the unknowns can be estimated.

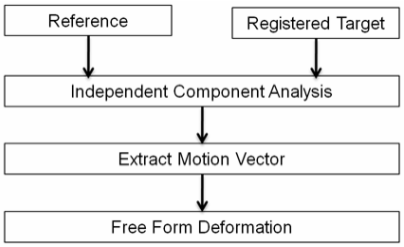

Fig. 2. Block diagram of ICA-based refinement.

To have the results be more computationally efficient, we employed the FastICA algorithm [20], which is an approximation method for ICA. This method basically generates a new contrast function by minimizing the mutual information and estimating the multidimensional source with the projection pursuit method. FastICA has been used for general-purpose data analysis and is 10 to 100 times faster than conventional ICA. The proposed ICA algorithm–based refinement step is summarized as follows.

First, we picked a 2D image from the target 3D volume image and saved the target slice number as S_{tar}. Then we picked n image slices from the reference image volume (slices from S_{tar}-(n/2) to S_{tar}+(n/2-1)). With these selected images (n images from the reference and 1 image from the target) ICA is calculated.

To measure the similarity of the features between target and reference images, we employed Euclidian distances. The reference slice, which has the minimum Euclidian distance from the target slice, was saved with its slice number (S_{ref}). Fig. 3 illustrates ICA planes from the reference and target slices. In this example, reference 2 (the dashed box) best matched the target slice.

We processed this method for each x, y, and z axis. This process was performed for all three axes (i.e. x, y, and z directions) so that 64 control points (four points for each axis direction) were acquired and used as transformation parameters in the next step.

The 3D slice numbers of each voxel image were converted to the 3D coordinates of the 64 control points. These coordinates of the control points inside each voxel image were used as a motion vector, so that the elastic transformation of the target image was conducted by free-

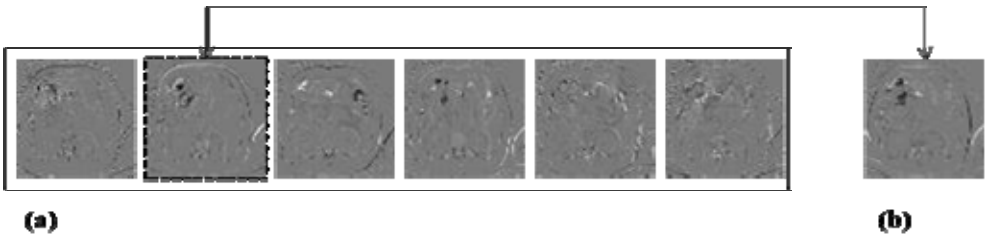

Fig. 3. Extracted feature from (a) reference slices and (b) the target slice. The dashed box indicates the best matching ICA slice of the target ICA slice, in this case, S_{ref} = 2.

form deformation (FFD) [16, 17].

2.3 GPU-based Acceleration

This image registration algorithm is a time-consuming process. To accelerate the processing time, parallel processing was applied. GPU-based acceleration has been widely used in a variety of applications because it is cost effective, easy to implement, and minimizes change in the original source codes. We used CUDA technology proposed by NVIDIA in both 3D affine transformation and free-form deformation, which are the most CPU-intensive processes in the proposed algorithm. We compare the results with and without parallel processing in Section 3.

In short, the process using a GPU can be described as follows.

(1) Define the three axes of the 3D image as the thread, block and ID of a grid for GPU processing.

(2) Allocate GPU memory and copy the 3D data from host to GPU memory.

(3) Calculate the coordinates of each transformed pixel by dividing a whole 3D affine transformation process into the multi-threads on the GPU.

(4) Merge the resulting coordinates of each thread in GPU memory.

(5) Copy the results from the GPU into host memory and free up GPU memory.

The graphics processing unit that we used was the GeForce GTX 260, which has 216 processing cores and 896MB of GDDR3 memory.

2.4 Image Data

We tested six image sets that consisted of five cases of non-Hodgkin's lymphoma (NHL) and one case of multiple myeloma (MM) scanned in KIRAMS. These data were obtained from six patients studied under the KIRAMS institutional review board–approved protocol for radio-immunotherapy evaluation. As mentioned, PET and CT images were acquired continuously on a combined PET/CT scanner (Siemens Biograph6). Each CT and PET image measured 512 × 512 × 274-324 and 128 × 128 × 274-324 voxels, respectively, and each slice of the images was a transverse view. The cubic voxel dimensions of the MR scanner (Siemens TrioTim 3T) were 364-379 × 831-1127 × 115-120, and each image slice was a T1-weighted image of a coronal view.

To match the different viewpoints between image sets, we transformed the axis of the MR images to a transverse view.

3. EXPERIMENTAL RESULTS

The proposed algorithm was implemented on a Linux machine with C++ and CUDA technology. To analyze the results easily, we also developed a 3D image viewer that can display the reference PET/CT, the target MR, and the resulting registered image in a window. It also has a function to change the viewpoint to coronal, transverse, and sagittal views.

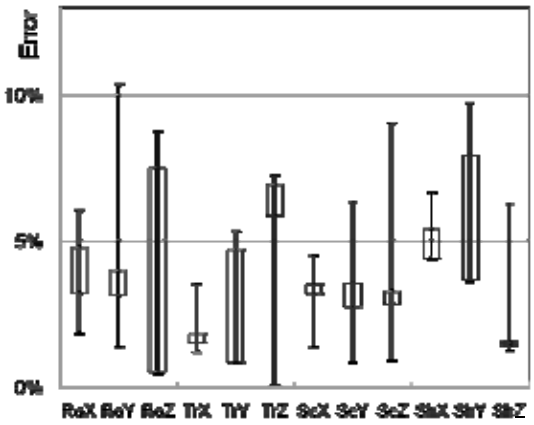

Fig. 4. Results of reproducibility test with PSO. Each plot represents the percentage error for 12 parameters of affine transformation (rotation: Ro, translation: Tr, scale: Sc and shear: Sh for three dimensions) using XCAT digital phantom image.

3.1 Particle Swarm Optimization

In NMI-based matching, PSO exhibited significantly reduced processing times, compared with the greedy search algorithm. With greedy search, the total number of parameter sets to be evaluated is about 0.35 million (only five varieties for each parameter set), which requires about 97 hours with an Intel Core i5 750 CPU and 8GB memory for a 128 × 128 × 128 pixel 3D XCAT [21] phantom image. In our experiments however, PSO took only 1.87 hours for registration of the 3D images.

Since PSO updates the next transformation parameters to calculate the cost function (i.e. NMI) by using a random number generator, the results of each registration may vary even when an experiment is performed. Thus, consistency in the results is one of the most important performance indicators in PSO. Although more iterations and particles in PSO produce more accurate results, we limited them to 400 iterations and 12 particles to take into account the trade-offs between performance and execution time. We repeated the test five times with the same images to investigate the reliability of the algorithm. Fig. 4 shows the deviation from ground truth. The results indicate that the transformation parameters obtained by PSO are consistent, and have fewer than 10% small variations.

3.2 NMI-based Global Matching

The proposed registration algorithm consists of two independent registration methods, NMI-based global matching and ICA-based refinement. The resulting image sets with each method were evaluated independently.

Fig. 5 shows the transverse view of the global matching results for two different patient cases. In these cases, the patient position and FOV were slightly different between reference and target images. The CT image and MR image show different organs and sizes, even in the same z-slice before registration. For case 1, the shape of the liver in the

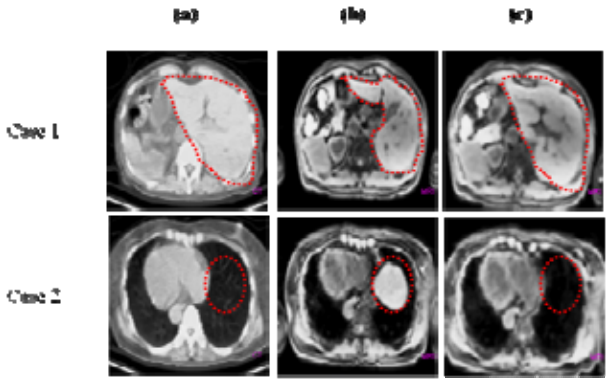

Fig. 5. Global registration results for two cases, where (a) is the reference CT, (b) is the target MR, and (c) is the MR after global registration.

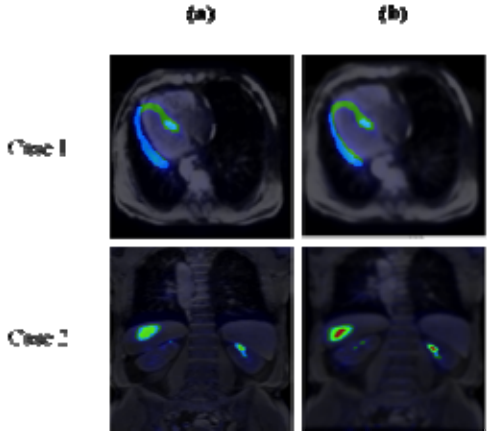

Fig. 6. Two cases with PET/MR fusion images for (a) global registration and (b) refinement.

CT image (a) and the MR image (b) were different before registration, but after global matching (c), the size and shape of the liver were considerably well registered. For case 2, unlike the CT image (a), the liver is shown in the MR image (b). In the registered MR image (c), the liver disappeared, and the size of the heart is quite analogous to the CT image.

3.3 ICA-based Refinement

Fig. 6 shows the results of ICA-based fine adjustment. Even after the global registration process, the CT and global-matched MR images have some discrepancies. When the PET image is overlaid on the global-registered MR image, without the proposed refinement step, we still observe some misalignment in the PET/MR fusion image (a). Case 3 is a transverse image of the heart area. The wall of the left ventricle is left-sided in the global-registered fusion image (a). After the ICA-based refinement, the PET/MR image shows that the misalignment has been considerably corrected (b). Case 4 is an image set of a patient with a suspicious region at the lower side of the liver. After the refinement process (b), the lesion of the region of interest was successfully matched in the PET/MR fusion image.

3.4 GPU-based Acceleration

The CUDA architecture exhibited a significant reduction in processing time. In this study, we compared the processing time of a GPU (Geforce GTX 260) with that of a CPU (AMD X2 64). It took 3.86 CPU seconds to transform a 3D image (128 × 128 × 128). The processing time was dramatically reduced to 0.396 seconds with the GPU. It shows that GPU-based parallel processing turns out to be about 9.7 times faster than CPU-based processing.

4. CONCLUSION

The aim of this study is to develop an image registration algorithm for abdominal PET/CT and stand-alone MR images. We developed a 3D elastic image registration algorithm that consists of NMI-based global matching and ICA-based refinement.

The NMI-based global matching algorithm adopted affine parameters for geometric transformation and NMI for similarity measurement. For efficient updates of the affine parameters, a particle swarm optimization method was adopted. In ICA-based refinement, ICA feature planes were utilized and matched to determine the motion vectors of 64 control points in a 3D space. Based on the control points, we transformed the target image elastically by B-spline–based freeform deformation. In addition, we accelerated the processing time via GPU-based parallel processing with the CUDA architecture so the processing time of the 3D transformation is dramatically improved.

To overcome shortcomings in the conventional intensity-based method, we developed an additional ICA-based refinement step. Performance of this proposed hybrid method was verified by matching PET/CT and MR images. Moreover, the reliability of this method will enable the algorithm to be utilized for CT-CT registration as well as CT-MR registration in the future. Furthermore, we expect the proposed algorithm will be applied to various combinations of multimodality imaging applications.

ACKNOWLEDGEMENTS

This work was supported by the Commercializations Promotion Agency for R&D Outcomes (COMPA) (No. 2014K000268), the National R&D Program through the Korea Institute of Radiological and Medical Sciences (No. 1711021927), and the National Research Foundation of Korea (No. NRF-2015M2B2A9028143) funded by the Ministry of Science, ICT & Future Planning of the Korean government.

References

[1] Medha V Wyawahare el al. “Image Registration

Techniques: An overview," *IJSIP*, Vol. 2, No. 3, pp. 11-28, Sep. 2009.
[2] Ramachandran Prabhakar el al., "An insight into PET-CT based radiotherapy treatment planning," *Cancer Therapy*, Vol. 5, pp. 519-524, 2007.
[3] Raj Shekhar et al., "Automated 3-dimensional elastic registration of whole-body PET and CT from separate or combined scanners," *Journal of Nuclear Medicine* , Vol. 46, No. 9, pp. 1488-1496, Sep. 2005.
[4] N Charnley et al., "The use of CT-MR image registration to define target volumes in pelvic radiotherapy in the presence of bilateral hip replacements," *British Journal of Radiology*, Vol. 78, No. 931, pp. 634-636, 2005. Article (CrossRef Link)
[5] J. Kang et al., "A small animal PET based on GAPDs and charge signal transmission approach for hybrid PET-MR imaging," *Journal of Instrumentation*, Vol. 6, No. 8, pp. P08012, Aug. 2011. Article (CrossRef Link)
[6] Jan Kybic and M Unser, "Fast parametric elastic image registration," *IEEE Transaction on Image Processing*, Vol. 12, Issue. 11, pp. 1427-1442, Nov. 2003. Article (CrossRef Link)
[7] Senthil Periaswamy and Hany Farid, "Medical image registration with partial data," *Medical Image Analysis*, Vol. 10. No. 3, pp. 452-464. 2006. Article (CrossRef Link)
[8] Rafael C Gonzalez and Richard E Woods, "Digital Image Processing. 3rd Edition," *Pearson Prentice Hall*, pp. 142-165, 2010.
[9] Josien P W Pluim et al., "Mutual information based registration of medical images: a survey," *IEEE Trans Med Imaging 2003*, Vol. 22, No. 8, pp. 986-1004, 2003. Article (CrossRef Link)
[10] C E Shannon, "A Mathematical Theory of Communication," *Bell System Technical Journal*, Vol. 27, No. 4, pp. 623-656, Oct. 1948. Article (CrossRef Link)
[11] M Bhattacharya and A Das, "Multi Resolution Medical Image Registration Using Maximization of Mutual Information & Optimization by Genetic Algorithm," *IEEE Nuclear Science Symposium*, Vol. 4, pp. 2961-2964, Oct. 26 2007-Nov. 3 2007. Article (CrossRef Link)
[12] Shun'ichi Kanekoa et al., "Using selective correlation coefficient for robust image registration," *Pattern Recognition*, Vol. 36, Issue. 5, pp. 1165-1173, May. 2003. Article (CrossRef Link)
[13] James Kennedy and Russell Eberhart, "Particle swarm optimization," *Proc. of the IEEE Int. Conf. on Neural Networks*, Vol. 4, pp. 1942-1948, Nov. 27 1995-Dec. 1 1995. Article (CrossRef Link)
[14] Russell Eberhart, "Micro Machine and Human Science, A new optimizer using particle swarm theory," *Proc. of the Sixth Int. Sym. on Micro Machine and Human Sci.*, pp. 39-43, Oct. 04 1995-Oct. 06 1995. Article (CrossRef Link)
[15] Petra A van den Elsen et al., "Medical image matching-a review with classification," *IEEE Engineering in Medicine and Biology*, Vol. 12, Issue. 1, pp. 26-39, Mar. 1993. Article (CrossRef Link)
[16] Thomas M. Lehmann et al., "Survey: Interpolation methods in medical image processing," *IEEE Transactions on Medical Imaging*, Vol. 18, Issue. 11, Nov. 1999. Article (CrossRef Link)
[17] D Rueckert et al., "Nonrigid registration using free-form deformations: application to breast MR Images," *IEEE Transactions on Medical Imaging*, Vol. 18, No. 8, pp. 712-721, Aug. 1999. Article (CrossRef Link)
[18] Derek L G Hill et al., "Medical image registration," *Physics in Medicine and Biology*, Vol. 46, No. 3, pp. R1-R45, 2001. Article (CrossRef Link)
[19] Aapo Hyvarinen and E Oja, "Independent component analysis: algorithms and applications," *Neural Networks*, Vol. 13, Issue. 4-5, pp. 411-430, Jun. 2000. Article (CrossRef Link)
[20] Aapo Hyvarinen et al., "Fast and Robust Fixed-Point Algorithms for Independent Component Analysis," *IEEE Trans. on Neural Networks*, Vol. 10, No. 3, pp. 626-634, May. 1999. Article (CrossRef Link)
[21] W P Segars et al., "Realistic CT simulation using the 4D XCAT phantom," *Med. Phys.*, Vol. 35, Issue. 8, pp. 3800, 2008. Article (CrossRef Link)
[22] Chui et al., "A new point matching algorithm for non-rigid registration," Computer Vision and Image Understanding, Vol. 89, No. 2-3, pp. 114-141, 2003. Article (CrossRef Link)
[23] Cachier et al., "3D non-rigid registration by gradient descent on a Gaussian-windowed similarity measure using convolutions," Proc. of IEEE Workshop on Mathematical Methods in Biomedical Image Analysis, pp. 182-189, Jun. 11 2000-Jun. 12 2000. Article (CrossRef Link)
[24] Hakjae Lee, "A study on medical image registration between PET-CT and PET-MR," MA thesis, KOREA University, Seoul, Korea, Dec. 2009.

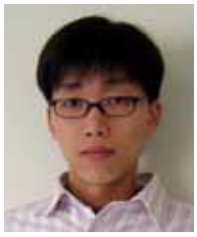

Hakjae Lee received a BSc in electric and electronic engineering from the Chung-Ang University in 2005 and an MSc and PhD in Bio-convergence Engineering from the Korea University in Seoul, Korea, in 2010 and 2014, respectively. Now, he is working for the research institute of Global Health Tech. at Korea University as a research professor. His research interests include medical image processing and radiation detector development for medical applications.

Jaehee Chun received a BSc in biomedical engineering from Korea University in 2015. Now, he is studying in the Department of Bio-convergence Engineering at Korea University as an MSc student. His research interests include medical image processing.

Kisung Lee received a BSc and an MSc in electronics engineering from the Korea University in 1990 and 1992, respectively, and a Ph.D. in elec-trical engineering from the University of Washington at Seattle in 2003. During 2005 to 2007, he was an assistant professor at Kongju National University, Korea. He has served as a reviewer for IEEE Transactions on Nuclear Science and IET Image Pro-cessing. He served as the Treasurer for the 2013 IEEE Science Symposium, Medical Imaging Conference and Workshop on Room-Temperature. He is now with the Department of Radiologic Science at Korea University and has worked in the area of radiation detectors, physics in x-ray and gamma-ray imaging systems, and image processing algorithms for medical applications.

Kyeong Min Kim received an MSc and Ph.D. from Hanyang University, Seoul, Korea, in 1995 and 1999, respectively. From 1999 to 2004, he was a research fellow in the department of radiology at the National Cardiovascular Center Research Institute, Osaka, Japan. He is currently a senior research scientist in the molecular imaging research center at the Korea Institute of Radiological and Medical Sciences, Seoul, Korea. His research interests include multi-disciplinary research related to medical imaging involving nuclear physics, imaging processing, and data mining.